IDA

INSTITUTE FOR DEFENSE ANALYSES

A Study of the Thermal Effects in a Smart Structure Helicopter Rotor

Armand Martin
Bohdan Balko
Michael A. Rigdon

July 1999

IDA Paper P-3435

Log: H 98-002588

PREFACE

This document was prepared in response to a task entitled "Materials Science Analyses." The analysis reported in this document was undertaken to provide a "ballpark" estimate of the temperatures that might be encountered when a piezoelectric actuation device is enclosed within a small cavity in a honeycomb sandwich structure. The dimensions utilized in the analysis are notional estimates and were not intended to model a specific application. The goal of this work was to determine whether or not thermal management for one possible configuration of smart materials is a design issue that should be considered by the research community.

CONTENTS

FIGURES

TABLE

I. INTRODUCTION

A meeting was held on February 24–25, 1998 at Boeing (St. Louis) to review the progress of the Defense Advanced Research Projects Agency (DARPA) Smart Structures Helicopter Rotor Demonstration Program for the purpose of determining its future technical direction. During the course of this meeting several concepts for demonstrating active noise and vibration control of helicopter rotors were described.

One concept being considered is a trailing edge flap driven by a high-displacement piezoelectric actuator device. A detail of one type of actuator is shown in Figure I-1. The actuator mechanism, shown in Figure I-1(a), is enclosed within a pocket cut from the honeycomb inside the rotor blade, as shown in Figure I-1(b). This activator requires an 800-V power supply and draws a current on the order of 0.3 A. Thus, depending on the duty cycle and efficiency of the mechanism, some portion of the 240 W of electrical input energy will be converted to heat. Since the DARPA meeting in February 1998, several different actuator designs have been proposed; however, the basic physical processes remain the same. One of this report's authors (M.R.) questioned whether the heat dissipated by these actuators could cause a problem within the close confines of the composite structure where they are to be located.

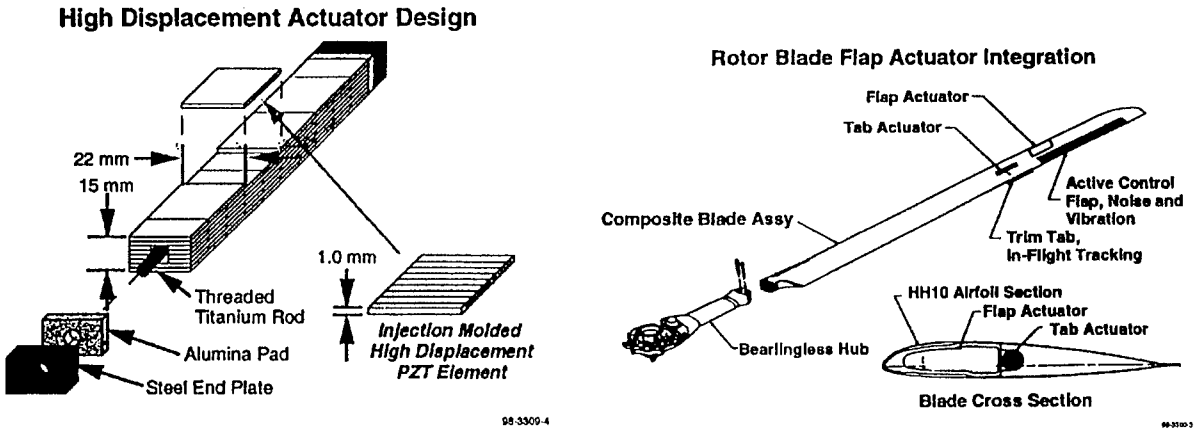

Figure I-1. Trailing Edge Flap Driven by a High-Displacement Piezoelectric Actuator Device

A quick study was undertaken by IDA to provide an initial estimate of the temperatures that may be encountered if no provisions are made for cooling the actuator.

The geometry and dimensions used in the following calculations are approximations based on concepts presented at the February meeting.

This report documents the results of this study and provides a ball-park estimate of the temperatures that may be encountered by the actuator and surrounding composite structure. Section II discusses the heat transfer calculation and describes the computer code, HEAT 8. Section III gives the results of our investigation, pertinent to the design and operation of the smart structure helicopter rotor.

II. HEAT TRANSFER CALCULATION

A. HEAT TRANSFER PROCESSES

To estimate temperatures for the actuator and surrounding composite structure, we must consider several sources of heat. In general, heat transfer between two solid regions of space separated by an air gap can occur by *conduction* through the air gap, *radiation* between the surfaces enclosing the air gap, and *convection* of the intervening air. In addition, we also have to consider heat generation and include heat sources which provide an additional minor complication. All of these processes are dealt with in a direct way in the code (HEAT 8).

In general, when treating radiation, we should also consider absorption of the radiated energy by the air molecules; as a practical matter, however, this can be shown to be negligible in our case and thus will not be considered in detail here. In what follows we describe how each of these processes is implemented in HEAT 8, which was originally designed to deal only with conduction (Landau and Lifshitz, 1959, and Anderson, 1989) but has been recently generalized to include the other processes important to our heat transfer problem.

B. CONDUCTION

Our treatment of conduction can be understood by reference to Figure II-1, where we show three adjacent cells which participate in the process.

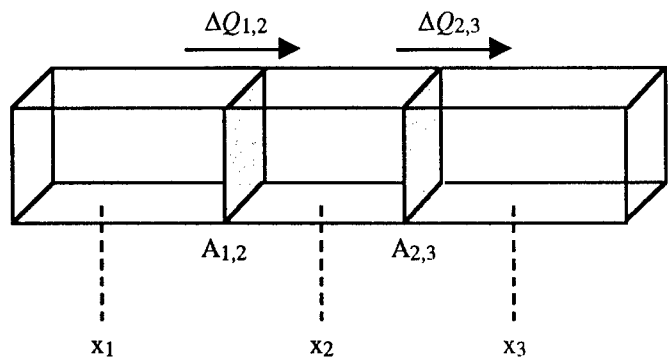

Figure II-1. Schematic Showing Three Cells Participating in Heat Conduction

The Fourier law of heat transfer states how much heat is transferred between two regions in space when a temperature difference exists between the regions. The law of mass action determines what the resultant temperature change is in these regions. In Figure II-1 an amount of heat $\Delta Q_{1,2}$ is transferred in time Δt from cell 1 to cell 2 and an amount of heat $\Delta Q_{2,3}$ is transferred between cells 2 and 3 as given by Equations 1 and 2. The resultant temperature change of cell 2 is obtained from the law of mass action as given by equation 3.

$$\Delta Q_{1,2} = \frac{k_{1,2}}{l_{1,2}} A_{1,2} (T_1 - T_2) \Delta t \quad , \tag{1}$$

$$\Delta Q_{2,3} = \frac{k_{2,3}}{l_{2,3}} A_{2,3} (T_2 - T_3) \Delta t \quad , \tag{2}$$

$$\Delta T_2 = (\Delta Q_{1,2} - \Delta Q_{2,3}) / \rho_2 C_2 V_2 \quad . \tag{3}$$

In these equations $k_{i,j}$, $l_{i,j}$, $A_{i,j}$, and $\Delta Q_{i,j}$ refer to the thermal conductivity, distance between cell centers i and j, surface area between cells i and j, and heat transferred between cells i and j, respectively. T_i, ρ_i, C_i, V_i, and ΔT_i represent the temperature, density, specific heat, volume, and temperature change of cell i..

C. RADIATION

In Figure II-2 we show three cells (1,2,3) separated by two surfaces, $A_{1,2}$ and $A_{2,3}$. We calculate the radiation emitted by these surfaces using the Stefan–Boltzman law of emission (Equation 4) and the law of mass action (Equation 5) to determine the resultant temperature change of cells 1 and 3. Absorption in the air contained in cell 3 is neglected.

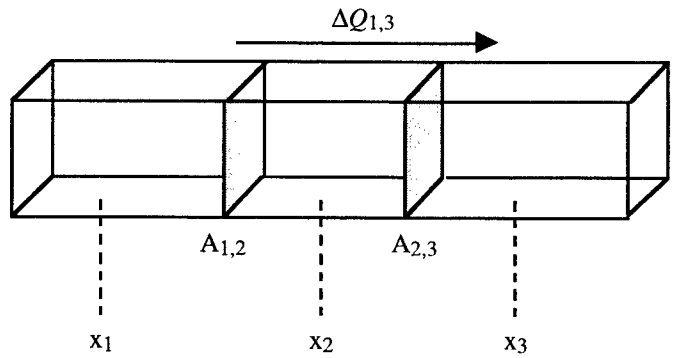

Figure II-2. Schematic Showing Radiative Heat Transfer between Two Walls

$$\Delta Q_{1,3} = A_{1,2} \cdot \sigma \cdot \varepsilon_{1,2} T_1^4 - A_{2,3} \cdot \sigma \varepsilon_{2,3} T_3^4 \quad , \tag{4}$$

$$\Delta T_1 = -\Delta Q_{1,3} / \rho_1 C_1 V_1 \quad , \tag{5}$$

$$\Delta T_3 = +\Delta Q_{1,3} / \rho_3 C_3 V_3 \quad , \tag{6}$$

where σ is the Stefan-Boltzman constant, $\varepsilon_{i,j}$ is the emissivity at the surface separating cells i and j, and the other parameters are as specified for Equations (1)–(3).

D. CONVECTION

A fluid can be in mechanical equilibrium even though it is not in thermal equilibrium, i.e., the temperature is not constant throughout the fluid. This situation, however, can also be unstable, leading to currents which tend to mix the fluid—a condition called convection. Convection can be a powerful heat transfer mechanism but not under all conditions.

The condition of stability (no convection) has been determined (Landau and Lifshitz, 1965) to be

$$\frac{\partial T}{\partial z} > -g/C_p \quad , \tag{7}$$

where T is the temperature in the fluid at point z, g is the acceleration due to gravity, and C_p is the specific heat.

Using Equation (7), we can estimate the minimum requirements for the onset of convection in our problem. Assuming a separation of l = 1 cm, with g = 980 cm/sec^2 and C_p = 0.24 (cal/gm/°C), we get less than 10^{-3} °C as the minimum temperature difference required for convection to set in. This temperature is easily exceeded in our system. Thus, although convection is possible in our problem, we must still determine the effectiveness of this heat transfer mechanism relative to the other heat transfer mechanisms.

For this estimate we use the empirical formula derived by Langmuir, which gives the heat transfer from a vertical surface at a temperature T_1 to the ambient air at a temperature T_2. This is given by

$$W = -9.3(\varphi_2 - \varphi_1)\ \text{W/cm}^2 \quad , \tag{8}$$

where φ_1 and φ_2 are parameters in the range of 0 to 0.0709 for a range of temperatures from 0 to 900 K. The actual values are provided in a table elsewhere (Anderson, 1989). A discussion of convection, with references to other theoretical and experimental work, is presented by Strong (1938).

From our runs, we estimate the temperature difference between the wall and the first air cell at steady state to be not more than about 10–20 K. Using Equation (8), this gives us about 0.01 to 0.02 W/cm^2 transferred due to convection. The transfer due to

radiation is about 1.75 W/cm^2 for a wall at 500 °F and the outer surface at 0 °F. From conduction the transfer is 0.135 W/cm^2 to a layer of air at the wall 0.01 cm thick.

The efficiency of convection depends on how much heat the air can hold, the temperature difference between the air and the two surfaces, and the velocity of the air movement. From the estimate above we expect the effect of convection on the result to be negligible compared to the other heat transfer modes, conduction and radiation. The estimates of convection effects were based on the assumption of natural convection. A more appropriate approach for dealing with the region inside a rapidly moving rotor blade may be to use a forced convection model. This would require detailed knowledge of the air space geometry in the rotors. At this point we do not have details of the rotor structure that would justify the use of a better model to estimate the contribution from convection. Thus, for this ball-park estimate, neglecting convection altogether is justified.

III. HEAT GENERATION AND TRANSFER IN THE SMART STRUCTURE ROTOR

A. DESCRIPTION OF THE PHYSICAL PROBLEM

Figure III-1 shows the physical model that we used in this study. This model is a simplification of the actuator in the rotor blade shown in Figure I-1, but it retains the basic features required for realistic analysis. The dimensions in Figure III-1 are representative of the typical geometry expected to be used and do not strictly adhere to what is shown in Figure I-1. The filament is between two plates that have infinite extent in both length and width. The filament, which represents the actuator, is made of ceramic, and the plates are made of fiberglass. In the space between the plates is still air, the temperature of which changes according to the dynamics of the problem. The space outside the plates is also air, but at a constant 70 °F, so that it constitutes a heat sink. This constant-temperature reservoir represents the fresh regions of air encountered by the moving blades. Actually, the moving air would heat the blades so that they would be at a higher temperature. We ignored this heating effect—which would only add to the perceived problem—and assume that the entire configuration is at a constant 70 °F initially and that the only modes for heat transfer from the filament are by radiation and conduction. Our goal is to calculate the maximum temperature of the filament as it is fed with electrical power.

B. DESCRIPTION OF THE COMPUTATIONAL MODEL

Based on the physical model shown in Figure I-1, we constructed the computational model shown in Figure III-2. We assume the length of the filament is small compared with the diameter and that the temperature only varies in the lane of Figure III-1, view 2. Therefore, the domain has two dimensions. Also, we need only to model one-fourth of the cross section (shown in the inset of Figure III-2) because of the obvious symmetry in the problem. Therefore, along the right and bottom sides of the mesh we have symmetric boundary conditions. We approximate the circular shape of the filament with a square located in the lower left-hand corner and composed of four cells. Each of the dashed blocks represents one element in the discrete model. The solid lines

show boundaries of the model and the boundaries for the transition from one material to another.

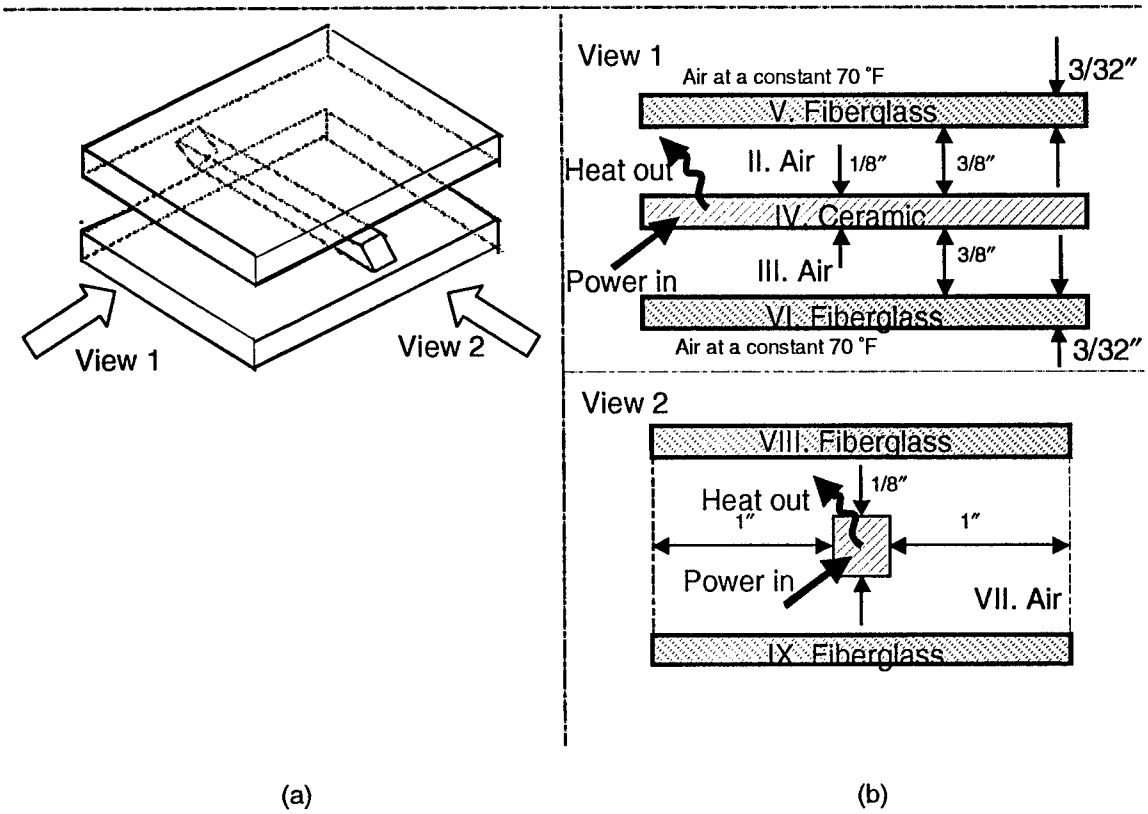

Figure III-1. Two Views of the Geometry of the Physical Structure. (a) Directions of the two views shown in (b) where two cross sections of the structure are presented

The material properties used in the computational model are given in Table I-1. Note that, lacking any specific information about the filament, we used the thermal properties of granite for this structure.

Table I-1. Material Properties for the Computational Model

Material (units)	Thermal Conductivity [Cal/(sec cm Kelvin)]	Density (g/cm^3)	Specific Heat [Cal/(g Kelvin)]
Air (20 °C and 0.46 ATM)	0.000270	0.000590	0.240
Glass	0.00280	2.40	0.20
Granite	0.0060	2.60	0.210

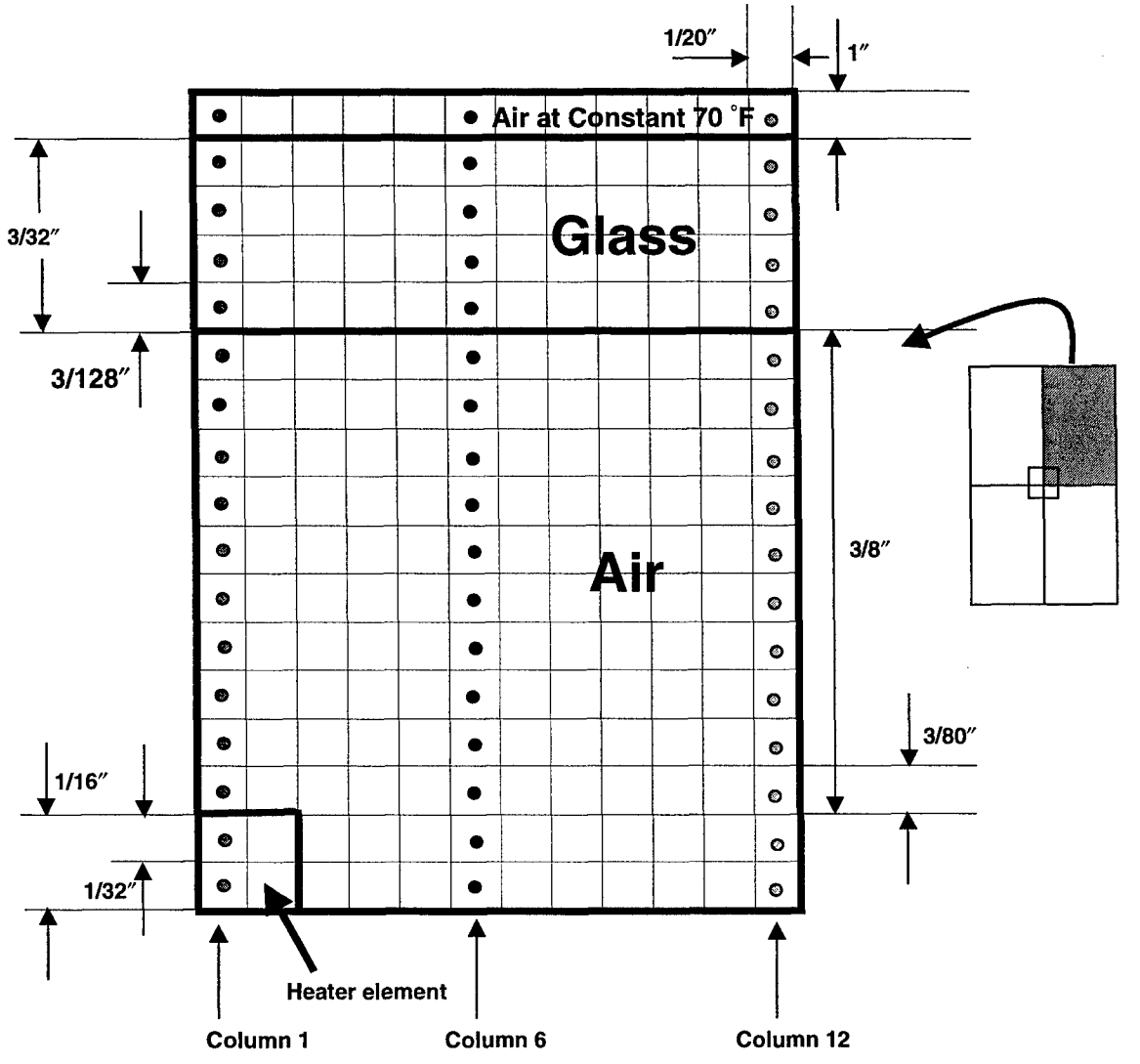

Figure III-2. A Picture of the Computational Model (not to scale)

C. RESULTS

Figure III-3 (a)–(d) shows the temperature at the center of the filament (or the average temperature of the cell) as a function of time for 1, 10, 25, and 50 W of input power, respectively. These plots of the filament temperatures show the time needed to reach steady state and the final maximum filament temperatures. We make several observations. First, the steady-state temperature does not increase linearly with input power. From these plots it is also clear (and it might be surprising at first) that as power increases, the time to steady state decreases. Figure III-4 shows the time to steady-state temperature for the various input powers. In this figure, the functional dependence of time to steady state on input power is not obvious, but clearly, the time to steady state decreases as input power increases.

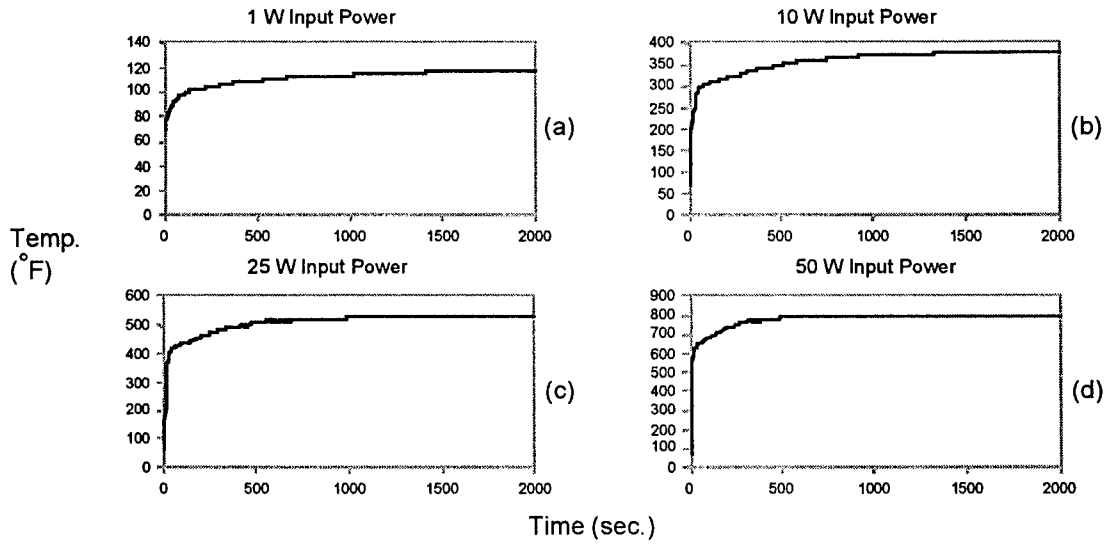

Figure III-3. Temperatures of the Filament for Various Input Powers

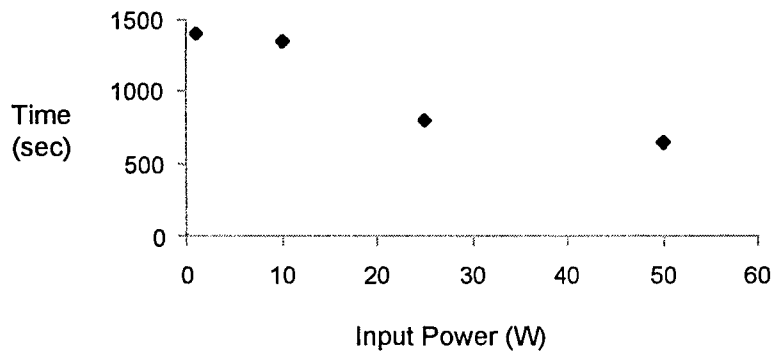

Figure III-4. Time to Steady-State Temperature for Various Input Powers

We can explain both these observations by noting that the heat transfer is dominated by radiation, as will become apparent with more results. Since radiation dominates, and the amount of heat transferred by radiation between two unobstructed points is proportional to the fourth power of the respective temperatures, we would expect nonlinear dependence with input power.

Figures III-5 and III-6 plot temperatures from the computational model against distance, for each column of elements (see Figure III-2), at three times during the computation. Figure III-5 is for 1 W input power; Figure III-6 is for 20 W input power. The three times of computation are 40, 500, and 1,970 sec; 1,970 sec corresponds to steady state.

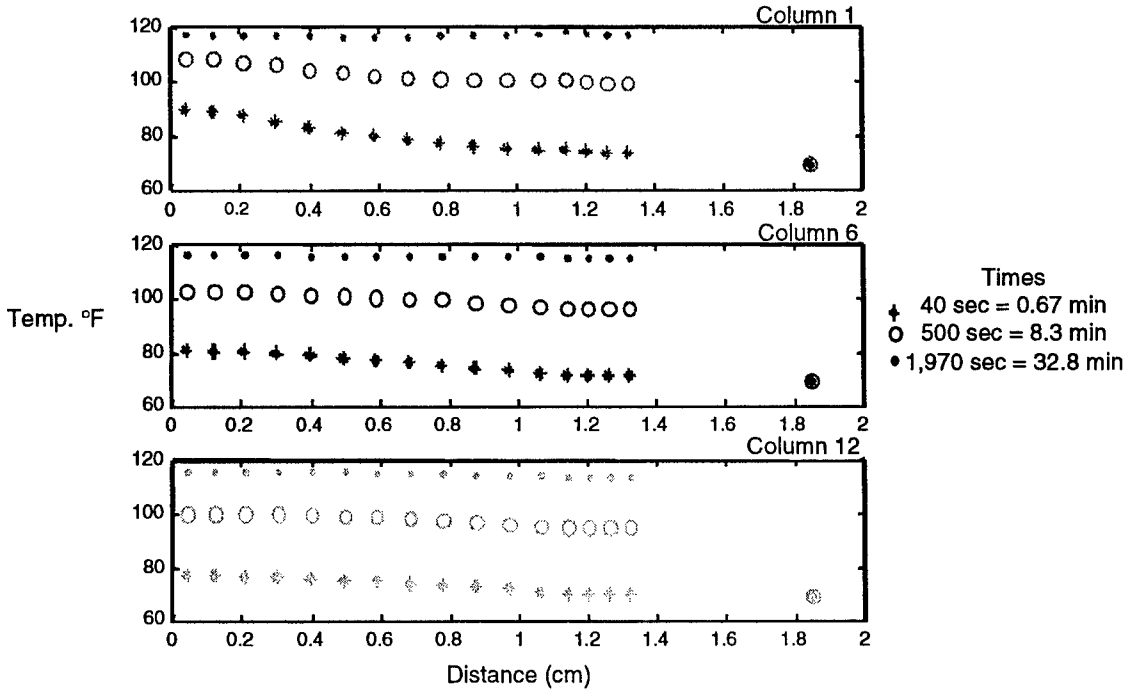

Figure III-5. Temperatures at Positions Shown in Figure III-2, for 1 W of Input Power

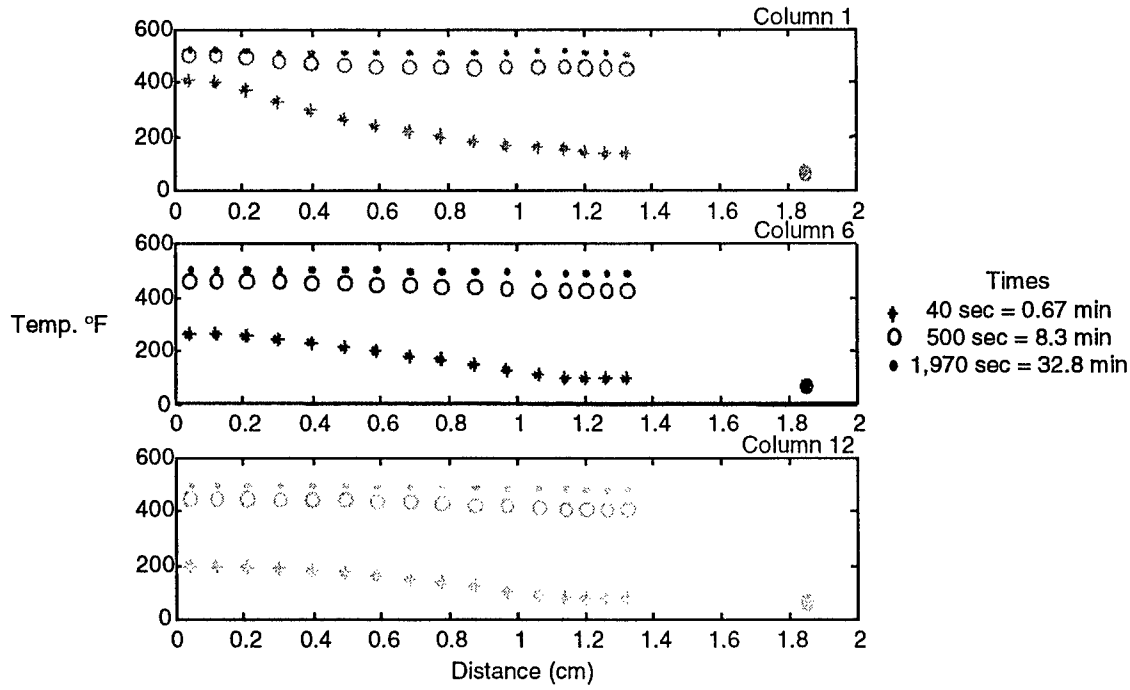

Figure III-6. Temperatures at Positions Shown in Figure III-2, for 20 W of Input Power

The most interesting feature of the plots in Figures III-5 and III-6 is the near-constant temperature distribution through the air inside the fiberglass (see Figure III-2). We would expect that if we did not include heat transfer by radiation that there would be a large temperature gradient through the air because air is an insulator. Therefore, we attribute the near-constant air temperature to the heat transfer by radiation. Thus, at steady state, the radiation keeps the outer wall of the filament and the inside wall of the fiberglass at nearly the same temperature and thus also the air between them.

Comparing Figures III-5 and III-6, we see that the temperature reaches steady state more quickly at the higher input power. In Figure III-6, the 500-sec plot is much closer to the 1,970-sec (steady state) plot than in Figure III-5.

Figure III-7 plots maximum filament temperatures as a function of input power with both radiation and conduction in the heat transfer problem and with only conduction. These curves clearly show that the heat transfer is dominated by radiation. For example, the plot of heat transfer with only conduction assumed shows a maximum filament temperature of well over 6,000 °F with 10 W of input power, while the plot of conduction with radiation shows a maximum temperature of 375 °F at 10 W input power.

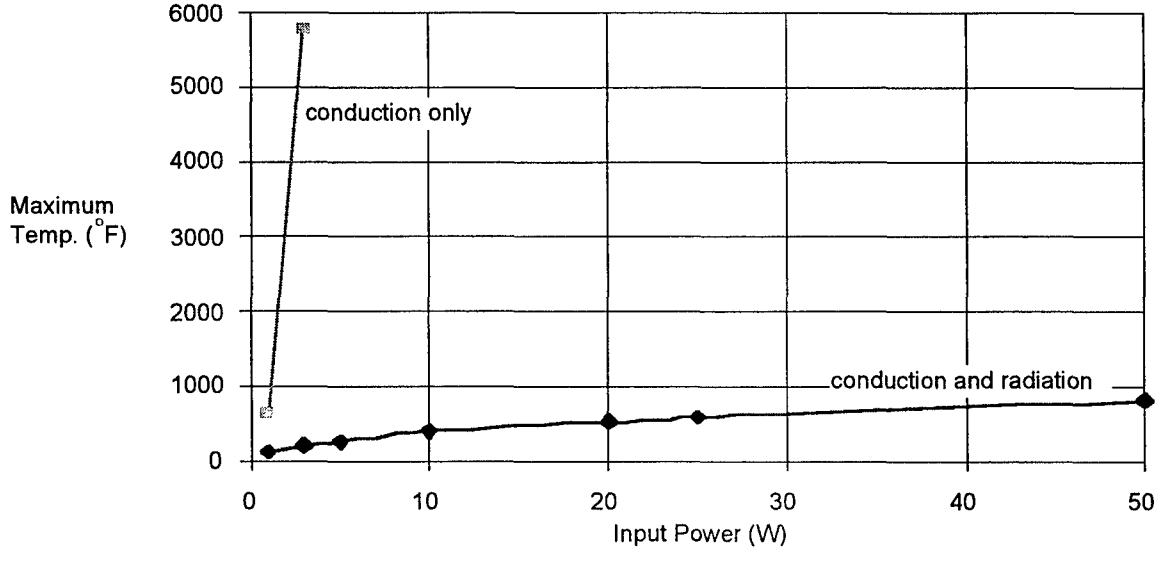

Figure III-7. Maximum Filament Temperatures with Conduction and with and without Radiation

Figure III-8 shows the dependence of maximum filament temperature with input power. As we stated above, because heat transfer from radiation is proportional to temperature to the fourth power, and because heat transfer for this problem is dominated by radiation, the curve is not linear.

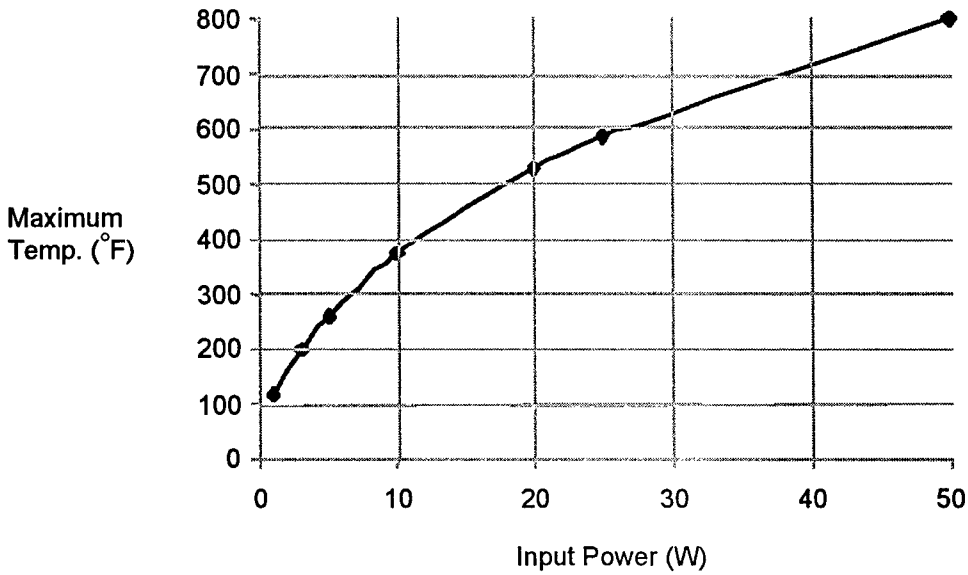

Figure III-8. Maximum Filament Temperature Taking into Account Conduction and Radiation

IV. SUMMARY AND CONCLUSION

We successfully modified a heat transfer code (HEAT 8), which was originally designed to deal with conduction only, to also include transfer by radiation. This code was selected because of certain advantages inherent in the direct application of physical phenomena in elementary form that is its basis. The code can handle multiple media and multiple effects such as heat conduction, molecular diffusion chemical reactions, and radiation. It can also easily handle complex structures and various geometric forms. The code does not currently account for heat transfer by convection. Because this mode may be important to consider in some situations, and because we may need to use the code in more general problems, we plan to investigate the inclusion of convection.

We applied the code to the smart-structure rotor problem, assuming a range of input powers (1 to 50 W) and 100-percent duty cycle, which covers the actual operating conditions of interest. For lower duty cycles, estimates can be made by assuming a reduced power. Our results show that for the powers considered, the temperature of the filament ranged from 120 °F to 800 °F, and the temperature of the inside surface of the surrounding fiberglass reached similar temperatures. These temperatures, especially at the higher ranges, could cause problems with the materials and should be of concern to the designers.

In our analysis we took into account the cooling effect of the movement of the rotor through the air by assuming that the air temperature outside the rotor was at a constant 70 °F. This heat sink effect essentially provided fresh air into which the rotor dumped the excess heat. There is an additional frictional heating that was neglected, which of course would increase the temperature above 70 °F. All of these effects can be treated more accurately in a more detailed study.

REFERENCES

Landau, L.D., and Lifshitz, E.M. (1959), *Fluid Mechanics,* London: Pergamon Press.

Anderson, H.L. (1989), *A Physicist's Desk Reference,* American Institute of Physics.

Carslaw and Jaeger (1969), *Conduction of Heat in Solids,* 2nd ed., Oxford University Press.

Balko, B., Berger, R.L. (1968), *Rev. Sci. Instr.,* Vol. 39, p. 498.

Balko, B., Berger, R.L., Anderson, K. (1981), *Rev. Sci. Instr.,* Vol. 52, p. 888.

Strong, J. (1938), *Procedures in Experimental Physics,* New York, Prentice-Hall, Inc., p. 505.

APPENDIX

METHOD OF ANALYSIS

APPENDIX
METHOD OF ANALYSIS

A. THE FINITE ELEMENT SIMULATION (FES) COMPUTATIONAL TECHNIQUE

The computational procedure adopted for this problem is Finite Element Simulation [Balko and Berger (1968), Balko, Berger, and Anderson (1981)]. The FES technique relies on the application of physical and chemical laws (usually in a form which permits easy generalization and application to complex structures) to the system under investigation in the following manner.

The system is divided into a number of convenient cells (labeled i, j, k), using the symmetry of the situation to minimize the number of geometrical parameters. Each cell is characterized by three types of parameters:

a. *Geometrical parameters* $g(\mathrm{i})$, such as the position of the center of a cell, its volume, cross sectional area, surface area, etc.

b. Physical parameters $p(\mathrm{i})$, such as diffusivity, specific heat, etc.

c. Transport functions $\tau(\mathrm{i})$, such as temperature, concentration, pressure, etc.

$\tau(\mathrm{i})$ is an intensive parameter, and the associated extensive parameters, e.g., heat, number of particles, are denoted $Q(\mathrm{i})$. The parameters in group (c) are specified initially [$\tau(\mathrm{i})$ at $t = 0$], and then a time interval Δt is chosen over which the calculation is to take place. The choice of Δt is governed by the requirement that it should be just small enough to prevent "overshoot" in the calculations.

The heart of the calculation is the set of physical laws which describe changes in the system parameters $\tau(\mathrm{i})$ over the interval $(t, t + \Delta\tau)$. A general process (m) can be thought of as causing a change $\Delta Q^m(\mathrm{i})$ due to the transfer parameter $\tau^m(\mathrm{i})$ of cell i. It can be calculated from

$$\Delta Q^m(\mathrm{i}) = \Omega\,(\mathrm{i}, \mathrm{i}+1)\cdot\Lambda(\mathrm{i}, \mathrm{i}+1)\cdot\Phi(\mathrm{i}, \mathrm{i}+1)\,\Delta t \quad , \qquad \text{(A-1)}$$

where Ω, Λ and Φ are functions of the appropriate geometrical, physical, and transfer parameters, respectively, of the system.

$\Delta Q^m(i)$ is a change in the extensive parameter corresponding to $\tau^m(i)$ and gives the amount of "material" transferred out of cell (i) by the process *m*. In the case of molecular diffusion, ΔQ is the number of molecules transported in time Δt due to concentration differences in the cells. In the case of heat conduction, ΔQ is the heat transported in time Δt due to the temperature differences in the cells. The changes in the transport functions can be obtained from

$$\Delta\tau^m i = \left(\Delta Q^m(i-1) - \Delta Q^m(i)\right) / R^m(i) \quad . \tag{A-2}$$

This leads to a new $\Delta\tau^m(i)$ by

$$\tau(i)_{new} = \tau(i)_{old} + \sum_{m=1}^{M} \Ädm(i) \quad , \tag{A-3}$$

where we have assumed (*M*) independent processes affecting the parameter $\tau(i)$.

The preceding three steps are repeated until t_{max} is reached. The result of the calculation is a profile of the τ parameter as a function of position (cell center) for different times. Note that this is a dynamic simulation calculation; to obtain an equilibrium situation, the temporal development has to be simulated until an asymptotic behavior is reached.

In this section we specialize the computational procedure FES to simulate the thermal time development of a complex systems with heat sources. Here we include a short description of how the calculations are done. In the next section we discuss the stability and resolution.

The system is divided into a number of convenient cells, each with a definite density ρ, thermal conductivity *K*, specific heat *C*, and diffusivity *D*. The temperature in each cell is specified initially, and then a time interval is chosen over which conduction is to take place.

Heat conduction during the time interval Δt takes place from one cell to the other according to Fourier's law of heat transfer. For cell (i) and (i – l), this is given by:

$$\Delta Q(i,i-1) = \frac{A(i,i-1)}{i(i,i-1)} K(i,i-1)(T_i - T_{i-1})\Delta t \quad , \tag{A-4}$$

where $A(i, i-1)$ is the area across which the transfer takes place, $K(i,i-1)$ the thermal conductivity between the cells, and $i(i, i-1)$ is the separation of the cell centers.

The temperature change in the ith cell after this transfer of heat between the ith cell and two neighboring cells (i – l) and (i + l) is

$$\Delta T_i = \left(\Delta Q(i,i-1) - \Delta Q(i,i+1)\right) / (C_i \rho_i V_i) \quad . \tag{A-5}$$

This type of program (algorithm) allows for relatively easy solutions to complicated, multilayered boundary problems. Another medium can be added without an appreciable increase in complexity of solutions, whereas in the usual numerical methods of solving the partial differential equation of heat conduction, addition of another medium complicates things immensely.

In addition to the passive heat transfer due to thermal diffusion, we can take account of heat sources in the cell i in a natural way by including in addition to ΔQ(i,i–l) the term ΔQ^H(i) = H(i,t) Δt, which gives the heat added in the cell i due to a reaction occurring in the cell or electrical current flowing through the cell.

B. STABILITY AND RESOLUTION

Before applying FES to study diffusion in complicated systems, we must be aware of two problems associated with numerical techniques.

1. Stability

In any computational scheme a certain time interval must elapse during which heat flows uninterruptedly between cells. If the Δt chosen is too large, then the equilibrium point will be passed and oscillations in the computed temperatures will lead to meaningless results. This is discussed in detail elsewhere (Carlslaw and Jaeger, 1969). The well-known condition which insures against such a blow-up is

$$XMOD = K\frac{\Delta t^2}{(\Delta X)} \leq 1/4 \quad ,$$

where ΔX is the effective linear dimension of the cell in question.

2. Spatial Resolution

One of the means of reducing *XMOD* below the required value is to increase the cell size. Doing so, however, tends to give us less partial resolution than may be desirable for a particular problem. The question also arises, what is the meaning of the temperature of the cell—is it the *average* temperature, the boundary temperature, or the *temperature* at the end point? Furthermore, is it necessary to know the number of cell divisions that should be made to obtain the desired resolution and accuracy? The general rule of thumb is (Carlslaw and Jaeger, 1969) that if S is the dimension of the material, a cell size of $S/6$ gives a "reasonable" solution. Each case must be handled separately, and we have found that sometimes one or two cell divisions give sufficiently good results.

C. CELL GEOMETRY

For a physical system in three dimensions, the most general approach would be to set up the diffusion equations (1) and (2) in three dimensions and allow for independent variations. However, it is often possible to use the symmetry of the problem to simplify the calculations. For physical problems which exhibit appropriate symmetry, rectangular, axial, or spherical coordinates may be used to advantage. For the specific system of coordinates, we need to use correct relations of area and volume.

For example, the area of a cell in these coordinates is given by

$$\text{Area} = \pi\,[2\,(r + \Delta r)]El \quad ,$$

where El = 0 for plane

= 1 for cylinder

= 2 for sphere

What is the required spatial resolution for the problem at hand?

There are two aspects to the resolution problem. First, there is the loss of resolution in FES due to the assumption that all the action takes place at definite centers of cells connected by thermal resistances. Thus, the temperature of each cell represents an average value of the temperature within the cell. The second problem involves the error introduced into the calculation by assuming that the temperature of each cell is constant over the whole region of the cell because it is clear that may not be the case. Carslaw and Jaeger (1969) remark that in practice division of the material of interest into six parts (cells) gives reasonable results. Although this is a good assumption, it may be too stringent for our purpose. We found that fewer cells also give good results, but the spatial resolution suffers.

REPORT DOCUMENTATION PAGE

Form Approved
OMB No. 0704-0188

1. AGENCY USE ONLY *(Leave blank)*	2. REPORT DATE	3. REPORT TYPE AND DATES COVERED
	July 1999	Final — March 1998 – September 1998

4. TITLE AND SUBTITLE
A Study of the Thermal Effects in a Smart Structure Helicopter Rotor

5. FUNDING NUMBERS
DASW01 94 C 0054
DASW01 97 C 0056
DARPA Assignment DA-2-1698

6. AUTHOR(S)
Armand Martin, Bohdan Balko, Michael A. Rigdon

7. PERFORMING ORGANIZATION NAME(S) AND ADDRESS(ES)
Institute for Defense Analyses
1801 N. Beauregard St.
Alexandria, VA 22311-1772

8. PERFORMING ORGANIZATION REPORT NUMBER
IDA Paper P-3435

9. SPONSORING/MONITORING AGENCY NAME(S) AND ADDRESS(ES)
Defense Advanced Research Projects Agency/DSO
3701 N. Fairfax Drive
Arlington, VA 22203

10. SPONSORING/MONITORING AGENCY REPORT NUMBER

11. SUPPLEMENTARY NOTES

12a. DISTRIBUTION/AVAILABILITY STATEMENT
Approved for public release; distribution unlimited (February 22, 2000)

12b. DISTRIBUTION CODE

13. ABSTRACT *(Maximum 180 words)*

One concept being considered for active noise and vibration control of helicopter rotors is a trailing edge flap design driven by a high-displacement piezoelectric actuator device. The proposed device requires an 800-V power supply and draws a current on the order of .3 A. Thus, depending on the duty cycle and efficiency of the mechanism, some portion of the 240 W of electrical input energy will be converted to heat. This study provides an initial estimate of the temperatures that may be encountered if no provisions are made for cooling the actuator. Also included are a discussion of the heat transfer calculation, assuming conduction and radiation as the dominant modes, and a description of HEAT 8, the computer code used.

14. SUBJECT TERMS
heat transfer, conduction, radiation, smart materials, helicopter rotor blades, piezoelectric actuators

15. NUMBER OF PAGES
26

16. PRICE CODE

17. SECURITY CLASSIFICATION OF REPORT	18. SECURITY CLASSIFICATION OF THIS PAGE	19. SECURITY CLASSIFICATION OF ABSTRACT	20. LIMITATION OF ABSTRACT
UNCLASSIFIED	UNCLASSIFIED	UNCLASSIFIED	SAR